JOURNAL OF GUIDANCE, CONTROL, AND DYNAMICS
Vol. 20, No. 3, May–June 1997

Constrained Steering Law of Pyramid-Type Control Moment Gyros and Ground Tests

Haruhisa Kurokawa*
Mechanical Engineering Laboratory, Ibaraki 305, Japan

A constrained steering law of pyramid-type control moment gyros (CMGs) is presented, and its procedure and implementation are detailed. The steering law uses a constraining relation of four input variables of the CMG system and solves nonredundant kinematics. Though the angular momentum workspace of this method is much smaller than the original maximum workspace, singularity avoidance is ensured, and this steering law is much simpler than usual steering laws. This method also can be applied to steering four of the six units of a MIR-type CMG system. Advantages of the steering law are verified against a gradient method and a singularity-robust-inverse steering law by using a ground-test facility simulating spacecraft motion. Moreover, operational modes of the law and a mode-switching procedure are evaluated experimentally.

Nomenclature

C = Jacobian matrix of the kinematic equation
C^* = Jacobian matrix of the constrained kinematic equation
$c\alpha$ = $\cos\alpha$
det = $\det(CC^t)$, singularity measure of the system
$\boldsymbol{H}$ = (H_x, H_y, H_z), total angular momentum vector of control moment gyro (CMG) system
h = angular momentum of CMG unit
$s\alpha$ = $\sin\alpha$
$\boldsymbol{T}$ = output torque of CMG system
α = $\cos^{-1}(1/\sqrt{3})$, skew angle of symmetric pyramid configuration
$\boldsymbol{\theta}$ = $(\theta_1, \theta_2, \theta_3, \theta_4)$
θ_i = gimbal angle of ith CMG unit

Introduction

A SINGLE-GIMBAL control moment gyro (CMG) system is a powerful torque generator for spacecraft attitude control. It has advantages over a double-gimbal CMG system and reaction wheels, in mechanical simplicity and higher output torque. Nonetheless, its control has an inherent problem with kinematic singularity. Once in a singular state, a CMG system cannot produce three-axis torque.

Singularity and control of general CMG systems have been studied theoretically by Margulies and Aubrun.[1] Many researchers, such as Yoshikawa[2] and Cornick,[3] have presented singularity avoidance techniques that use a null motion, moving the CMGs without torquing the vehicle. Simulations have demonstrated that this technique is effective for double-gimbal CMGs, though not always for single-gimbal CMGs (especially for the pyramid-type CMG system, which was most commonly studied). Tokar and Platonov[4] and Kurokawa[5] demonstrated that impassable singularities of general CMG systems can obstruct continuous control locally. Bauer[6] showed difficulties in global control of the pyramid-type system. Thereafter, Kurokawa[7] presented a problem in which exact and strictly real-time control is impossible for a certain large range of angular momentum space of the symmetric pyramid-type system.

Three types of methods have been proposed that may cope with these problems. The first permits some error in the output torque. Bedrossian et al.[8] used the singularity-robust(SR)-inverse method, which minimized this error as well as the gimbal rates. The second type of method uses a path planning technique. Paradiso[9] presented a tree search method for global steering if the future path of the CMG angular momentum is given before the maneuver control. Vadali and Krishnan[10] presented a suboptimal planning with regard to the feedback control of the spacecraft. The last type of method tries to maintain the exactness of the steering law in strict real-time performance, but restricts its operational range. Vadali et al.[11] presented a set of preferred initial gimbal angles that was guaranteed to avoid singularities for a limited class of maneuvers. Kurokawa's method[7] not only is a smooth extension of the latter method but also has repeatability and calculation simplicity. In addition, the method has three modes, each of which is effective for attitude control in one direction orthogonal to the others.

Evaluation of a steering law has usually been made by numerical simulations, and sometimes by using a real mechanism that simulated spacecraft motion. Vadali and Krishnan[10] used a platform supported by a spherical air bearing. Suzuki et al.[12] developed a ground-test station that was supported on conventional ball bearings, and tried robust attitude control using a CMG system.

This paper presents the implementation details of this method and demonstrates its performance by using a ground-test facility in comparison with other steering laws. The results showed that the proposed steering law is simple, requires no extra planning process, and ensures exact, real-time control. In addition, application of the proposed method to the control of a MIR-type CMG system is described.

Constrained Steering Law of Pyramid-Type CMG System

It has been shown that exact and strictly real-time control of the symmetric pyramid CMG system is only possible for a restricted workspace of angular momentum.[7] An example of such a steering law was proposed. Advantages of this steering law are repeatability, simplicity, and availability of modes. Based on these results, implementation details—as well as the mode switching process—are described in this section.

Constrained System and Restricted Workspace

The gimbal axes $\boldsymbol{g}_i$ of the pyramid-type CMG system are arranged normal to the surface of regular octahedron (Fig. 1). The system has four input variables θ_i whose origins are defined when angular momentum vector of each unit, $\boldsymbol{h}_i$, is on the square in the x-y plane in Fig. 1. The following constraining function makes the system nonredundant:

$$\theta_1 - \theta_2 + \theta_3 - \theta_4 = 0 \tag{1}$$

This constraint was applied so that it preserves symmetry about z axis and can be regarded as an appropriate extension of scissoring of CMG pairs. This condition is satisfied by the following, where $\boldsymbol{\theta}$ is a function of three-component vector $\phi = (\chi_i)$:

$$\boldsymbol{\theta} = (\chi_1 + \chi_2, \chi_1 + \chi_3, \chi_1 - \chi_2, \chi_1 - \chi_3) \tag{2}$$

Received June 10, 1996; presented as Paper 96-3790 at the AIAA Guidance, Navigation, and Control Conference, San Diego, CA, July 29–31, 1996; revision received Nov. 29, 1996; accepted for publication Dec. 7, 1996.

*Senior Researcher, Applied Physics and Information Science Department, 1-2 Namiki, Tsukuba. Member AIAA.

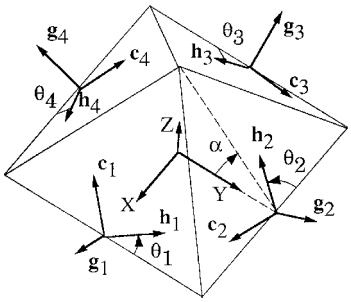

Fig. 1 Schematic of a pyramid-type system.

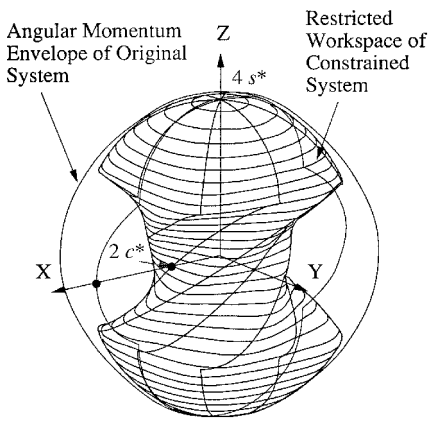

Fig. 2 Approximation of the reduced workspace under the constrained steering law.

Then the kinematic equation of this constrained system is given as follows:

$$\boldsymbol{H} = \boldsymbol{H}(\theta) = h \begin{pmatrix} -c\alpha \cos\chi_1 \sin\chi_2 + \sin\chi_1 \sin\chi_3 \\ -\sin\chi_1 \sin\chi_2 - c\alpha \cos\chi_1 \sin\chi_3 \\ s\alpha \sin\chi_1 (\cos\chi_2 + \cos\chi_2) \end{pmatrix} \tag{3}$$

This kinematic function, with restricted domain of variable χ, can be one-to-one and onto in a certain range of $\boldsymbol{H}$, which approximately forms a two-lobe workspace (Fig. 2). Because the boundary of this space cannot be defined uniquely, its cutting section by a plane normal to the z-axis is approximated here by

$$(H_x, H_y) = -2(c\alpha vp - uq, up - c\alpha vq)^t \tag{4}$$

where

$$u = H_z/(2s\alpha),\ v = \sqrt{1-u^2},\ p = \sqrt{\sin u},\ q = \sqrt{\cos u}$$

This workspace has the same maximum size as the original unconstrained system in the z direction, and about one-third the size in either the x or the y direction. As long as $\boldsymbol{H}$ is inside the workspace, gimbal angles can be determined uniquely and continuously as one of the solutions of Eq. (3). Uniqueness and continuity ensure not only singularity avoidance, but also the repeatability of the control. Repeatability is important for standard attitude maneuvers, such as a scanning motion. A conventional steering law (e.g., a gradient method) does not possess this characteristic.[7]

Steering-Law Process

In actual implementation, numerical inversion of Eq. (3) is inappropriate because of nonlinearity. Therefore, the steering law was realized as a solution of linear equations that are obtained by differentiation of Eq. (3):

$$\boldsymbol{T} = -hC \frac{\mathrm{d}\boldsymbol{\theta}}{\mathrm{d}t} = -hC^* \frac{\mathrm{d}\phi}{\mathrm{d}t} \tag{5}$$

The Jacobian matrix C^* of this constrained system is given by

$$C^* = \begin{pmatrix} c\alpha s\chi_1 s\chi_2 + c\chi_1 s\chi_3 & -c\alpha c\chi_1 c\chi_2 & s\chi_1 c\chi_3 \\ -c\chi_1 s\chi_2 + c\alpha s\chi_1 s\chi_3 & -s\chi_1 c\chi_2 & -c\alpha c\chi_1 c\chi_3 \\ s\alpha c\chi_1 (c\chi_2 + c\chi_3) & -s\alpha s\chi_1 s\chi_2 & -s\alpha s\chi_1 s\chi_3 \end{pmatrix} \tag{6}$$

where $\sin\chi_i$ and $\cos\chi_i$ are abbreviated as $s\chi_i$ and $c\chi_i$.

In real situations, the constraint condition in Eq. (1) is not guaranteed because the values of the gimbal rates derived from Eq. (5) are used for a finite sampling time and are not renewed continuously. To cope with this, feedback control was adopted in which null motion of the original system was added to make the residual [i.e., the left of Eq. (1)] vanish. Null motion for such a four-unit system has 1 degree of freedom and is generally obtained as $k\boldsymbol{\omega}_N$:

$$\boldsymbol{\omega}_N = ([\boldsymbol{c}_2\ \boldsymbol{c}_3\ \boldsymbol{c}_4],\quad -[\boldsymbol{c}_3\ \boldsymbol{c}_4\ \boldsymbol{c}_1],\quad [\boldsymbol{c}_4\ \boldsymbol{c}_1\ \boldsymbol{c}_2],\quad -[\boldsymbol{c}_1\ \boldsymbol{c}_2\ \boldsymbol{c}_3]) \tag{7}$$

where $\boldsymbol{c}_i$ is a row vector of the original Jacobian matrix C and $[\boldsymbol{a}\ \boldsymbol{b}\ \boldsymbol{c}]$ denotes the box product of three vectors.[1]

For stable feedback, the parameter k is determined with an appropriate feedback gain a as follows:

$$k = -a(\theta_1 - \theta_2 + \theta_3 - \theta_4)(\omega_{N1} - \omega_{N2} + \omega_{N3} - \omega_{N4})/|\boldsymbol{\omega}_N|^2 \tag{8}$$

Finally, the gimbal angle rates $\mathrm{d}\boldsymbol{\theta}/\mathrm{d}t$ are

$$\frac{\mathrm{d}\boldsymbol{\theta}}{\mathrm{d}t} = -\frac{1}{h} \begin{pmatrix} 1 & 0 & 1 \\ 0 & 1 & 1 \\ 1 & 0 & -1 \\ 0 & 1 & -1 \end{pmatrix} C^{*-1}\boldsymbol{T} + k\boldsymbol{\omega}_N \tag{9}$$

Computation of this steering law is composed of calculation of Eqs. (2–9), except Eq. (4). Because the variable transformations between $\boldsymbol{\theta}$ and ϕ and the feedback control process are very simple, and the Jacobian matrix C^* is a 3×3 matrix, the total calculation is much simpler than the usual steering laws (such as a gradient method or the SR-inverse method, which need a pseudoinverse calculation of a 3×4 matrix). In the real implementation for the ground test, code size of this steering law and calculation time were about two-thirds and one-half of those of a gradient method, respectively.

Note that this steering law is effective only in the restricted workspace. Therefore, an appropriate momentum management using Eq. (4) is required to keep $\boldsymbol{H}$ in the workspace.

Steering-Law Modes

There are five other constrained systems that have similar properties to the constrained system described in the preceding sections.[7] They have their own constraint conditions, kinematic equations, ranges of the variables, and workspaces. One of the five systems is a mirror image of the original constrained system about the x–z plane. The remaining four systems are obtained by $\pm\frac{2}{3}\pi$ rotations about $\boldsymbol{g}_1$ to the original system and its mirror image. The steering law for each of these systems remains exact and simple.

The six constrained systems make three pairs. These pairs are called modes and termed M1, M2, and M3. The workspace of each pair has a shape similar to that shown in Fig. 2, and the dominant direction lies along the z axis for the M1 mode, along $(1, 1, 0)^t$ for the M2 mode, and along $(1, -1, 0)^t$ for the M3 mode. The nominal gimbal angles, which correspond to $H = (0, 0, 0)^t$ are of the form of $(\gamma, -\gamma, \gamma, -\gamma)$, where $\gamma = 0$ or π for the M1 mode, $\pi/3$ or $-2\pi/3$ for the M2 mode, and $-\pi/3$ or $2\pi/3$ for the M3 mode. Because the dominant directions of all of the workspaces are orthogonal to each other, attitude control performance will be improved by introducing mode switching.

The steering law based on Eqs. (3–9) corresponds to the M1 mode. The steering law of other modes is obtained by applying the appropriate $\boldsymbol{H}$ and $\boldsymbol{\theta}$ coordinate transformations.

Mode Switching

Different modes share a region in $\boldsymbol{H}$ space inside of which we can select and change modes. When it is required to change the steering-law mode, gimbal angles must be changed to satisfy another constraint while keeping the same $\boldsymbol{H}$. There is, however, no continuous path from $\boldsymbol{\theta}$ of one mode to $\boldsymbol{\theta}$ of another mode without a change in $\boldsymbol{H}$, except for $\boldsymbol{H} = 0$. [When $\boldsymbol{H} = 0$, there exists a mode connection path given by $\boldsymbol{\theta} \propto (1, -1, 1, -1)$.] Therefore, operations such as feedback attitude control should be deferred until the switching process is completed.

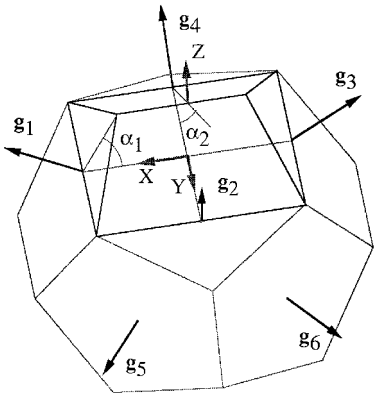

Fig. 3 Four-out-of-six unit system of MIR-type system.

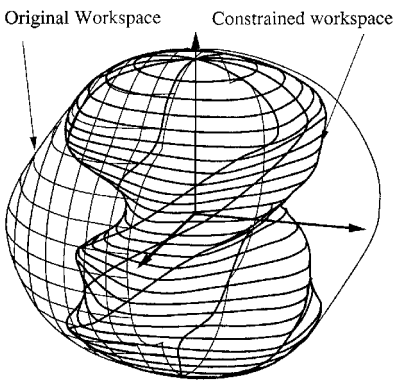

Fig. 4 Restricted workspace of a constrained MIR-type system.

In the experiments, the following simple method was applied. Here, one specifies a condition such that $\boldsymbol{H}$ is on the dominant direction of the newer mode (e.g., the z axis of the M1 mode). The gimbal angle for $\boldsymbol{H}$ along the z axis is acquired by a direct inverse calculation of Eq. (3), as follows:

$$\chi_1 = \sin^{-1}(H_z/2sa), \qquad \chi_2 = \chi_3 = 0 \tag{10}$$

The simplest way of changing $\boldsymbol{\theta}$ from the current to the preceding is a motion along a line.

This gimbal motion causes undesired torque but its effect can be made small. Because $\boldsymbol{H}$ is the same for the initial and the final θ in the CMG coordinate frame, the initial and the final angular momentum of the spacecraft alone may be similar when this motion is made fast enough. Thus, this motion will result in small deviation of the spacecraft's attitude and this deviation can be easily corrected by the feedback attitude control once the mode is changed.

Control of MIR-Type System

The concept of the constrained control can be applied to a MIR-type CMG system. The MIR-type system consists of six single-gimbal CMGs, symmetrically arranged on surfaces of a dodecahedron. In the usual operation, only four of the units are simultaneously driven. Any four-unit subsystem forms a congruent configuration, which can be regarded as a deformed pyramid configuration in which two units have a skew angle $\alpha_1 (= \sin^{-1}\sqrt{\{\frac{1}{2}[1 + \cos(\pi/5)]\}})$ and the other two, a skew angle $\alpha_2 (= \pi/2 - \alpha_1)$ (Fig. 3). Because the kinematic equation of this system is similar to Eq. (1), the same constraining condition as Eq. (2) can be applied and nonredundant kinematics similar to Eq. (3) can be obtained. This constrained system has a restricted workspace (Fig. 4), inside which exact steering is ensured. Of course, this configuration is not rotationally symmetric about any gimbal axis, so there is no additional mode.

Ground Experiment

Facility

The ground-test facility (Fig. 5) simulated the attitude dynamics of a spacecraft. The main truss structure holds devices such as CMG units, CMG driver circuits, balance adjusters, and a computer. The total weight is about 250 kg and the principal moments of inertia are 38, 38, and 42 kg m^2.

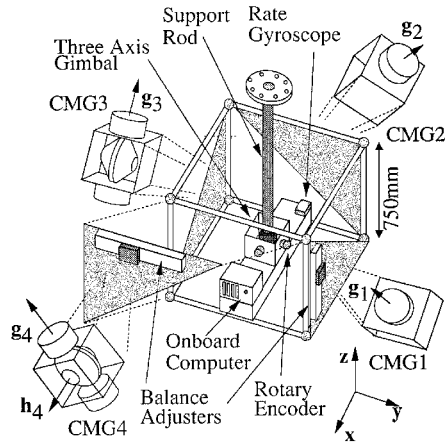

Fig. 5 Experimental test rig showing the center-mount suspending mechanism.

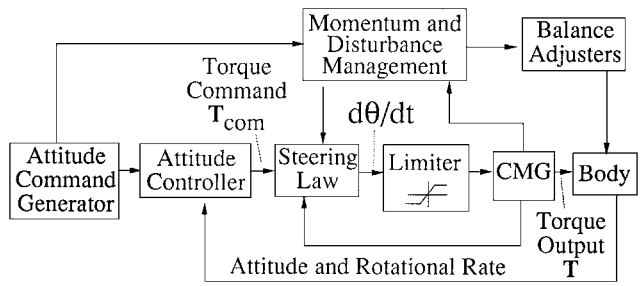

Fig. 6 Block diagram of the control system.

The entire system is suspended from the ceiling by a three-axis gimbal mechanism in its center. If the center of the gimbal coincides with the body's center of gravity, no torque appears at any orientation as a result of the gravitational force. In this way, motion in space can be simulated. This was achieved by using three balance adjusters, which can adjust the weight distribution along three orthogonal directions. The body's rotation was measured by three rotary encoders on the supporting gimbal and three rate gyros.

The main torquer was a pyramid-type single-gimbal CMG system designed and constructed at the Mechanical Engineering Laboratory. Each of four CMGs has a flywheel (13-mm diam, rotating at 5000 rpm). The angular momentum of each CMG is 3.8 Nms. The gimbal rate was limited to 1.0 rad/s by software, which resulted in 3.8 Nm maximum output torque. Because the CMG system can generate much larger torque than the friction torque of the supporting gimbal bearings, transient motion (such as a rapid maneuver) can be simulated well.

All attitude-control and steering-law processes were installed in an onboard computer equipped with i80386S×16 MHz CPU and i80387 floating point units (FPU). The calculation interval of each control cycle was set to 12 ms. All power was supplied from the laboratory by a pair of thin wires, which cause little disturbance force.

Attitude Controller

The block diagram of the control system is shown in Fig. 6. In the attitude controller, orientation of the test rig was represented by the vector component $\boldsymbol{\beta}$ of the Euler parameter.[13] An exact linearization method was applied[12] and two types of linear controllers were implemented. One was designed by using the "model matching method," which made the system's input/output transfer function match the desired function.[12] Another was a tracking controller, which followed a given trajectory of attitude change in terms of its first and second time derivatives. By using this, CMG motion can be specified to be as fast as possible without saturation of the gimbal rates.

Experimental Procedure

The test procedure can be outlined as follows: First, the body was controlled at a nominal attitude of $\boldsymbol{\beta} = (0, 0, 0)$ by using only the balance adjusters along with the PID (proportional-integral-derivative) controller. Thereafter, the CMG control started with a sequence of

attitude commands. The balance adjusters were controlled so that they generated an expected disturbance torque.

Experimental Results

In the following sections, steering laws used in experiments are arranged starting from a gradient method,[3] its extension with transpose steering law, SR-inverse method,[8] "preferred gimbal angles,"[11] and finally the proposed constrained method. Performance of the last will be shown step by step. These steering laws are abbreviated as follows; GM, GM*, SR, CM for a gradient method, its extension, the SR-inverse method, and the constrained method, respectively. The objective function of the GM was $\det(CC^t)$.

Angular Momentum Accumulation to the x Axis

Three experiments were carried out to demonstrate how singularity avoidance, such as the SR-inverse method, works. By setting an initial state, $\boldsymbol{\theta} = (0, 0, 0, 0)$, the balance adjusters were controlled so that a constant disturbance torque about the $(1, 1, 0)^t$ direction was generated while the body was under pointing control. Three steering laws were used: GM in experiment (Ex.) 1, GM* in Ex. 2, and SR in Ex. 3. GM* includes an additional singularity avoidance process given by the transpose steering law, in which the gimbal rate is calculated using transposed Jacobian rather than its pseudoinverse, when the system is near a singularity condition (i.e., when the determinant of the Jacobian matrix is smaller than a certain value).

Three components of $\boldsymbol{\beta}$ are shown in Fig. 7. As a constant disturbance torque was applied to the body, the CMG system tried to generate countertorque. The motion of Ex. 1 (indicated by gray lines in Fig. 7), indicates the output torque of the CMG system vanished by approaching an "impassable" singularity condition at $t = 18$ s followed by body rotation. On the contrary, the other two methods successfully avoided this singularity by generating some undesired torque.

Rotation About the z Axis

Experiments demonstrated the performance of preferred gimbal angles[11] compared with the SR-inverse steering law. The preferred gimbal angles for maneuver about the z axis are given as $\boldsymbol{\theta} = (0, 0, 0, 0)$.

Three experiments were made: Ex. 4 by GM from $\boldsymbol{\theta} = (0, 0, 0, 0)$, Ex. 5 by GM* from $\boldsymbol{\theta} = (-\pi/3, \pi/3, -\pi/3, \pi/3)$, and Ex. 6 by SR from the same $\boldsymbol{\theta}$ as Ex. 5. The command sequence of these experiments consisted of two maneuver motions, in which the z-axis component of reference attitude β_3 was changed twice. It was first rotated 36 deg about the z axis, then restored to the initial orientation after 10 s (Fig. 8a).

All of the results are shown in Fig. 8. In Ex. 4, the CMG system did not approach any singular point (Fig. 8c), and smooth maneuver resulted (Fig. 8a). On the contrary, the CMG system approached a singular point at $t \approx 2.3$ s in Exs. 5 and 6 (Fig. 8c). At that time, H_z saturated at smaller value than that of the maximum in Ex. 4 (Fig. 8b). Thus, it is shown that appropriate selection of initial gimbal angles, such as the preferred gimbal angles, is important for this kind of maneuver.

Note that SR failed singularity avoidance in Ex. 6. Possible reasons of this may be either that there are several singular surfaces crossing the z axis near this $\boldsymbol{H}$, or that avoidance motion of the SR was not fast enough to catch up with the command change.

Maneuver After Momentum Accumulation

Two experiments by CM and GM for the same control command were performed to demonstrate the repeatability problem of the usual gradient method. The control sequence consisted of five parts.

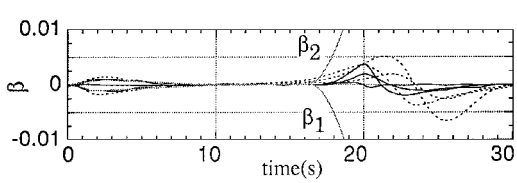

Fig. 7 Experiments showing performance of the singularity avoidance: · · · · ·, Ex. 1 (GM); ——, Ex. 2 (GM*); and - - - -, Ex. 3 (SR).

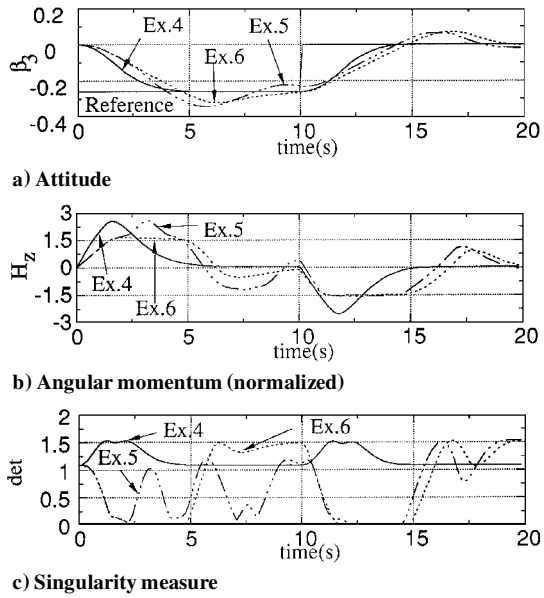

Fig. 8 Results of z-axis maneuver in Exs. 4 (GM), 5 (GM), and 6 (SR).

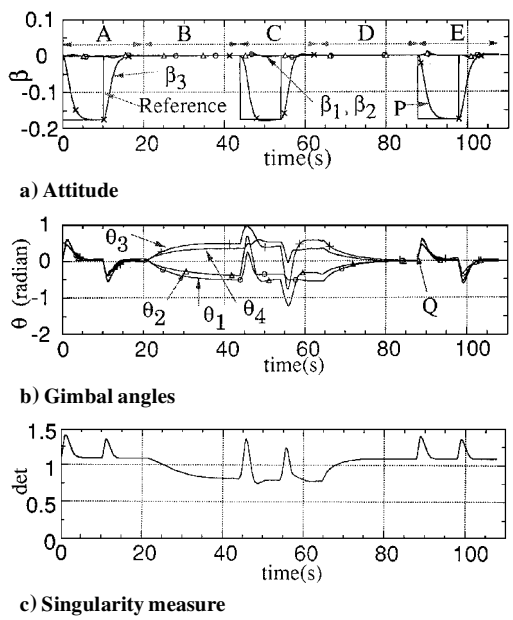

Fig. 9 Results of Ex. 7, maneuvers by the CM.

The z axis component of the reference orientation β_3 is shown in Fig. 9a. The other two components were fixed at zero. The first part of the sequence is a maneuver about the z axis, shown as part A in Fig. 9a. This command is similar to that of the previous three experiments. In part B in Fig. 9a, a disturbance torque was applied by the balance adjusters to move $\boldsymbol{H}$ to $(0.6, 0.4, 0.)^t$, while keeping the orientation of the body constant. (Note that these values of the angular momentum as well as those appearing later are normalized values.)

The third part (indicated by C) is the same as the first part. In part D, disturbance in the opposite direction was applied to return $\boldsymbol{H}$ to its origin, similarly to part B. Finally, the maneuver as of part A was repeated (E in Fig. 9a).

Two experiments (Ex. 7 by CM and Ex. 8 by GM) were performed. The results of these are shown in Figs. 9 and 10, respectively. The motions of the first three parts of the two experiments were almost the same. In the fourth part, however, motions of $\boldsymbol{\theta}$ were different. The gimbal angle $\boldsymbol{\theta}$ returned to the original in the case of CM (Q in Fig. 9b) but to a different point in the case of GM (S in Fig. 10b). This is because the local maxima of $\det(CC^t)$ were discontinuous somewhere during this motion. As a result, the last part was successful by CM (P in Fig. 9a) but not by GM (R in Fig. 10a). In the case

of GM, the determinant decreased and $\boldsymbol{H}$ saturated by hitting or approaching some singular surface (U and V in Fig. 10c).

These results clearly show that usual GM does not have repeatability that the CM has. Repeatability of this method is advantageous even for such a simple maneuver.

Mode Switching

Experiment 9 was conducted to evaluate the modes of CM and mode switching process. The trajectory tracking controller was used for this experiment.

The target trajectory can be seen in Fig. 11a. The experiment consisted of the following motions. First, the M1 mode was used. A maneuver with constant acceleration and deceleration about the z axis (part A in Fig. 11a) was planned by a smooth trajectory. After the first maneuver, a disturbance was applied in part B so that the angular momentum was accumulated to $(0.5, 0.5, 0.)^t$. Then, in part C, the z-axis maneuver was repeated. Next, the mode was changed to the M2 mode in part D. The new principal axis was in the $(1, 1, 0)^t$ direction. In part E, a maneuver was performed about this new direction. In part F, another disturbance was applied to accumulate $\boldsymbol{H}$ to $(1.2, 0.8, 0.)^t$. Finally, the maneuver about the $(1, 1, 0)^t$ direction was repeated in part G. Motions of $\boldsymbol{H}$ in parts E, F, and G were so planned that $\boldsymbol{H}$ moved out of the workspace of the M1 mode.

The results are shown in Fig. 11. The first three parts, A, B, and C, show motion similar to that in the previous experiment. As was desired by the tracking control, an almost constant magnitude of torque was generated in the periods of constant acceleration/deceleration (Fig. 11b).

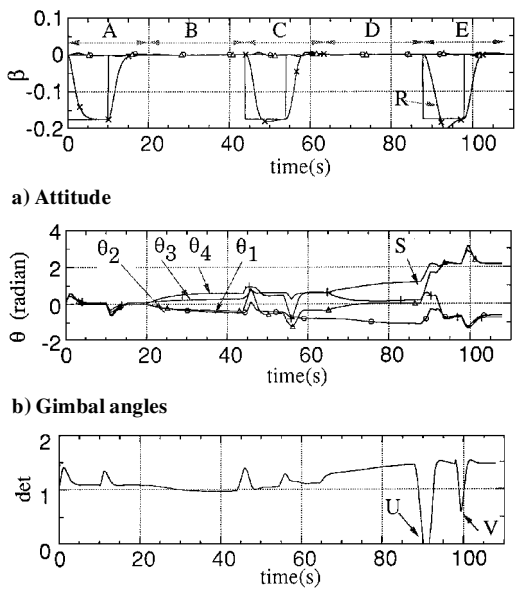

a) Attitude

b) Gimbal angles

c) Singularity measure

Fig. 10 Results of Ex. 8, maneuvers by the GM.

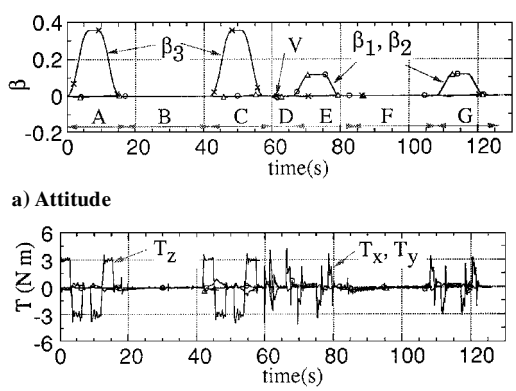

a) Attitude

b) Torque output

Fig. 11 Results of Ex. 9, tracking control with mode changing by CM.

In part D, the mode was changed from the M1 to the M2 while the attitude control was switched off. There was slight attitude deviation of the body due to undesired output torque (V in Fig. 11a). However, the attitude control immediately following this motion easily corrected this deviation. The last two maneuver motions, shown in parts E and G in Fig. 11, were successful and the system did not meet any singularity.

Summary of Experiments

It was shown that singularity avoidance such as the SR-inverse steering law is sometimes effective (Exs. 2 and 3), and sometimes not (Exs. 5 and 6). By these results, it is observed that the method of preferred gimbal angles is effective. This, however, is not adequate as the results of Exs. 7 and 8 show, but repeatability is also important. The results of Ex. 7 indicate that repeatability is realized by the proposed steering law.

The last experiment demonstrated the availability of modes and a feasible method of mode switching. Experiment 9 demonstrated that overall workspace size can be expanded by combining several modes.

Conclusions

A constrained steering law for the symmetric pyramid-type CMG system was proposed in detail and implemented on an onboard computer. The attitude control experiments on the ground verified that the proposed method was simple, i.e., faster and smaller in code size, and that it has advantages over other steering laws in assured ability of singularity avoidance and repeatability of control. The flexibility of workspace switching was also verified by the experiments. It also was shown that the concept of constrained control is applicable to a four-out-of-six subsystem of the MIR-type CMG system.

Nevertheless, further studies are required to find another constraint condition, smooth mode switching without impulsive torque, and mode switching without restriction.

References

[1]Margulies, G., and Aubrun, J. N., "Geometric Theory of Single-Gimbal Control Moment Gyro System," *Journal of the Astronautical Sciences*, Vol. 26, No. 2, 1978, pp. 159–191.

[2]Yoshikawa, T., "A Steering Law for Three Double Gimbal Control Moment Gyro System," NASA-TM-X-64926, 1975.

[3]Cornick, D. E., "Singularity Avoidance Control Laws for Single Gimbal Control Moment Gyros," *Proceedings of the AIAA Guidance and Control Conference* (Boulder, CO), AIAA, New York, 1979, pp. 20–33 (AIAA Paper 79-1698).

[4]Tokar, E. N., and Platonov, V. N., "Singular Surfaces in Unsupported Gyrodyne Systems," *Cosmic Research*, Vol. 16, No. 5, 1979, pp. 547–555.

[5]Kurokawa, H., "A Study of CMG Systems—for Selection and Evaluation," *Proceedings of 16th International Symposium on Space Technology and Science* (Sapporo, Japan), AGNE Kikaku, Tokyo, Japan, 1988, pp. 1243–1249.

[6]Bauer, S. R., "Difficulties Encountered in Steering Single Gimbal CMG's," Draper Lab., Space Guidance and Navigation Memo 10E-87-09, Cambridge, MA, 1987.

[7]Kurokawa, H., "Exact Singularity Avoidance Control of the Pyramid Type CMG System," *Proceedings of the AIAA Guidance, Navigation, and Control Conference* (Scottsdale, AZ), AIAA, Washington, DC, 1994, pp. 170–180.

[8]Bedrossian, N. S., Paradiso, J. A., Bergmann, E., and Rowell, D., "Steering Law Designs for Redundant SGCMG Systems," *Journal of Guidance, Control, and Dynamics*, Vol. 13, No. 6, 1990, pp. 1083–1089.

[9]Paradiso, J. A., "Global Steering of Single Gimballed Control Moment Gyroscopes Using a Directed Search," *Journal of Guidance, Control, and Dynamics*, Vol. 15, No. 5, 1992, pp. 1236–1244.

[10]Vadali, S. R., and Krishnan, S., "Suboptimal Command Generation for Control Moment Gyroscopes and Feedback Control of Spacecraft," *Proceedings of the AIAA Guidance, Navigation, and Control Conference* (Scottsdale, AZ), AIAA, Washington, DC, 1994, pp. 637–646.

[11]Vadali, S. R., Oh, H. S., and Walker, S. R., "Preferred Gimbal Angles for Single Gimbal Control Moment Gyros," *Journal of Guidance, Control, and Dynamics*, Vol. 13, No. 6, 1990, pp. 1090–1095.

[12]Suzuki, A., Kurokawa, H., and Kokaji, S., "Robust Attitude Control Using a CMG System and an Experiment with a Simulation Platform," *Proceedings of 12th IFAC Automatic Control in Aerospace* (Ottobrunn, Germany), 1992, pp. 197–202.

[13]Kane, T. R., Likins, P. W., and Levinson, D. A., *Spacecraft Dynamics*, McGraw–Hill, New York, 1983, pp. 12–16.